

# Validation of the MadAnalysis 5 implementation of ATLAS-SUSY-13-05

Guillaume Chalons (LPSC Grenoble)

*email: chalons@lpsc.in2p3.fr*

October 27, 2014

## Abstract

In this note we summarise our validation of the ATLAS search for direct third generation in final states with missing transverse momentum and two b-jets in  $\sqrt{s} = 8$  TeV [1].

## 1 Description of the implementation of the analysis

The analysis was implemented using the `MadAnalysis5 v1.1.11` framework [2] using for detector simulation `delphesMA5tune`. To validate the implementation of the analysis we generated  $10^5$  events for four benchmark points, used in [1] and further referred to:

- **8TeV\_b300\_n200**: in this scenario the lightest sbottom  $\tilde{b}_1$  is the only coloured sparticle contributing to the production process and it only decays via  $\tilde{b}_1 \rightarrow b\tilde{\chi}_1^0$ . The mass of the  $(\tilde{b}_1, \tilde{\chi}_1^0)$  pair is  $(m_{\tilde{b}_1}, m_{\tilde{\chi}_1^0}) = (300, 200)$  GeV.
- **8TeV\_b350\_n320**: the scenario is the same as above except that the mass of the  $(\tilde{b}_1, \tilde{\chi}_1^0)$  pair is  $(m_{\tilde{b}_1}, m_{\tilde{\chi}_1^0}) = (350, 320)$  GeV.
- **8TeV\_b500\_n1**: the scenario is the same as above except that the mass of the  $(\tilde{b}_1, \tilde{\chi}_1^0)$  pair is  $(m_{\tilde{b}_1}, m_{\tilde{\chi}_1^0}) = (500, 1)$  GeV.
- **8TeV\_t250\_c155\_n150**: in this scenario the only coloured sparticle is the lightest stop  $\tilde{t}_1$  and decays exclusively to  $\tilde{t}_1 \rightarrow b\tilde{\chi}_1^\pm$ . The subsequent decays of the  $\tilde{\chi}_1^\pm$  are invisible since the splitting between the  $\tilde{\chi}_1^\pm$  and the  $\tilde{\chi}_1^0$  is small  $\Delta m = m_{\tilde{\chi}_1^\pm} - m_{\tilde{\chi}_1^0} = 5$  GeV. The mass of the  $(\tilde{t}_1, \tilde{\chi}_1^\pm)$  pair is  $(m_{\tilde{t}_1}, m_{\tilde{\chi}_1^\pm}) = (250, 155)$  GeV.
- **8TeV\_t500\_c105\_n100**: this scenario is the same as above except that we have  $(m_{\tilde{t}_1}, m_{\tilde{\chi}_1^\pm}) = (500, 105)$  GeV.
- **8TeV\_t500\_c120\_n100**: this scenario is the same as above except that we have  $(m_{\tilde{t}_1}, m_{\tilde{\chi}_1^\pm}) = (500, 120)$  GeV and  $\Delta m = m_{\tilde{\chi}_1^\pm} - m_{\tilde{\chi}_1^0} = 20$  GeV.

- **8TeV\_t500\_c420\_n400**: this scenario is the same as above except that we have  $(m_{\tilde{t}_1}, m_{\tilde{\chi}_1^\pm}) = (500, 420)$  GeV.

Two sets of SRs, denoted by SRA and SRB, were defined to provide sensitivity to the kinematic topologies associated with the two sets of SUSY mass spectra. SRA is then further divided according to different  $M_{CT}$  thresholds:  $M_{CT} < 150, 200, 250, 300, 350$  GeV. SRA targets signal events with large mass splittings between the squark and the neutralino, therefore the benchmark points 8TeV\_b500\_n1 and 8TeV\_t500\_c105\_n100 are concerned, whereas SRB is designed to enhance the sensitivity when the squark-neutralino mass difference is small, hence benchmark points 8TeV\_b300\_n200 and 8TeV\_t250\_c155\_n150 are targeted.

The event samples were generated using `MadGraph5_v1.4.8` [3] and passed to `Pythia6.4` (with the PDF set `CTEQ6L1`) within `MadGraph` through the `pythia-pgs` package. The parameter cards in the form of `slha` files were provided by the ATLAS collaboration. We used our own cards for the rest. The  $x_q^{cut}$  parameter needed for the merging is defined as  $m_{\tilde{q}}/4$  where  $m_{\tilde{q}} = m_{\tilde{t}_1}, m_{\tilde{b}_1}$ . The generated files in the `StdHep` format were then passed through detector simulation using the modified version of `DELPHES3` [4] as implemented in `MadAnalysis5`. At the level of the detector simulation we used the “medium” selection criteria for electrons [5]. The “medium” selection criteria should be defined as the electrons identification efficiency times the reconstruction and track quality efficiency, however, we set the latter directly to 100% for simplification as it around 97-99%.

All the rest of the detector simulation is set as default as provided in the standard `DELPHES` card for ATLAS. We did not implemented the criteria on the charged  $p_T$  fraction ( $f_{ch}$ ) and on the fraction of the energy contained in the electromagnetic layers of the calorimeter ( $f_{em}$ ). The number of events was rescaled to a luminosity of  $20.1\text{fb}^{-1}$  using the tabulated 8 TeV stops/sbottoms production cross sections with squarks and gluinos decoupled <https://twiki.cern.ch/twiki/bin/view/LHCPhysics/SUSYCrossSections8TeVstopsbottom>.

## 2 Results and plots

We present in this section the tentative reproduction of the official plots provided in [1]. We first discuss SRA and then SRB.

### 2.1 Signal Region A (SRA)

The official distributions provided are the  $M_{CT}$  distribution (more details can be found in [6, 7]) with all selection cuts except the  $M_{CT}$  requirement, and the invariant mass of the b-jet pair  $m_{bb}$  with all selection cuts except the  $m_{bb}$  requirement. The computation of the special kinematic variable  $M_{CT}$  was done using the publicly available library which can be downloaded from <http://projects.hepforge.org/mctlib>. The results are displayed in Figure 1.

We now compare our cutflows with the official ones given in Table. 1 and 2. These cutflows

have been generated for the following benchmarks

$$SRA : \begin{cases} (m_{\tilde{b}_1}, m_{\tilde{\chi}_1^0}) = (500, 1) \text{ GeV} \\ (m_{\tilde{t}_1}, m_{\tilde{\chi}_1^\pm}, m_{\tilde{\chi}_1^0}) = (500, 120, 100) \text{ GeV} \end{cases} \quad (1)$$

$\tilde{b} \rightarrow b\tilde{\chi}_1^0$ (500/1) cutflow				
for SR $SRA$ , High $\Delta M$ , $E_T^{\text{miss}} > 150$ GeV				
cut	# events (scaled to $\sigma$ and $\mathcal{L}$ )	relative change	# events (official)	relative change (official)
Initial number of events	1737.4	1737.4	1738	1738
$E_T^{\text{miss}} > 80$ GeV filter	1627.9	-6.3%	1606.0	1606.0
Lepton veto	1592.6	-2.2%	1505.0	-6.3%
$E_T^{\text{miss}} > 150$ GeV	1370.3	-14.0%	1323.0	-12.1%
Jet Selection	122.2	-91.1%	119.0	-91.0%
$M_{bb} > 200$ GeV	99.3	-18.7%	96.0	-19.3%
$M_{CT} > 150$ GeV	83.5	-15.9%	82.0	-14.6%
$M_{CT} > 200$ GeV	68.3	-18.2%	67.0	-18.3%
$M_{CT} > 250$ GeV	50.5	-26.1%	51.0	-23.9%
$M_{CT} > 300$ GeV	33.4	-33.9%	35.0	-31.4%
$M_{CT} > 350$ GeV	19.0	-43.1%		

Table 1: Cutflow for the benchmark point  $\tilde{b} \rightarrow b\tilde{\chi}_1^0$  (500/1) in the Signal Region  $SRA$ , High  $\Delta M$ ,  $E_T^{\text{miss}} > 150$  GeV.

$\tilde{t} \rightarrow b\tilde{\chi}_1^\pm$ (500/120/100) cutflow				
for SR <i>SRA</i> , High $\Delta M$ , $E_T^{\text{miss}} > 150$ GeV				
cut	# events (scaled to $\sigma$ and $\mathcal{L}$ )	relative change	# events (official)	relative change (official)
Initial number of events	1737.4	1737.4	1738	1738
$E_T^{\text{miss}} > 80$ GeV filter	1582.2	-8.9%	1632.0	1632.0
Lepton veto	1140.8	-27.9%	1061.0	-35.0%
$E_T^{\text{miss}} > 150$ GeV	910.8	-20.2)/%	859.0	-19.0%
Jet Selection	39.6	-95.7%	39.0	-95.5
$M_{bb} > 200$ GeV	31.9	-19.4%	32.0	-18.0%
$M_{CT} > 150$ GeV	25.9	-18.8%	26.8	-16.2%
$M_{CT} > 200$ GeV	19.6	-24.3%	20.2	-24.6%
$M_{CT} > 250$ GeV	12.6	-35.7%	13.2	-34.7%
$M_{CT} > 300$ GeV	6.9	-45.2%	7.7	-41.7%
$M_{CT} > 350$ GeV	3.2	-53.6%		

Table 2: Cutflow for the benchmark point  $\tilde{t} \rightarrow b\tilde{\chi}_1^\pm$  (500/120/100) in the Signal Region *SRA*, High  $\Delta M$ ,  $E_T^{\text{miss}} > 150$  GeV. 100 000 signal events were generated for the cutflow.

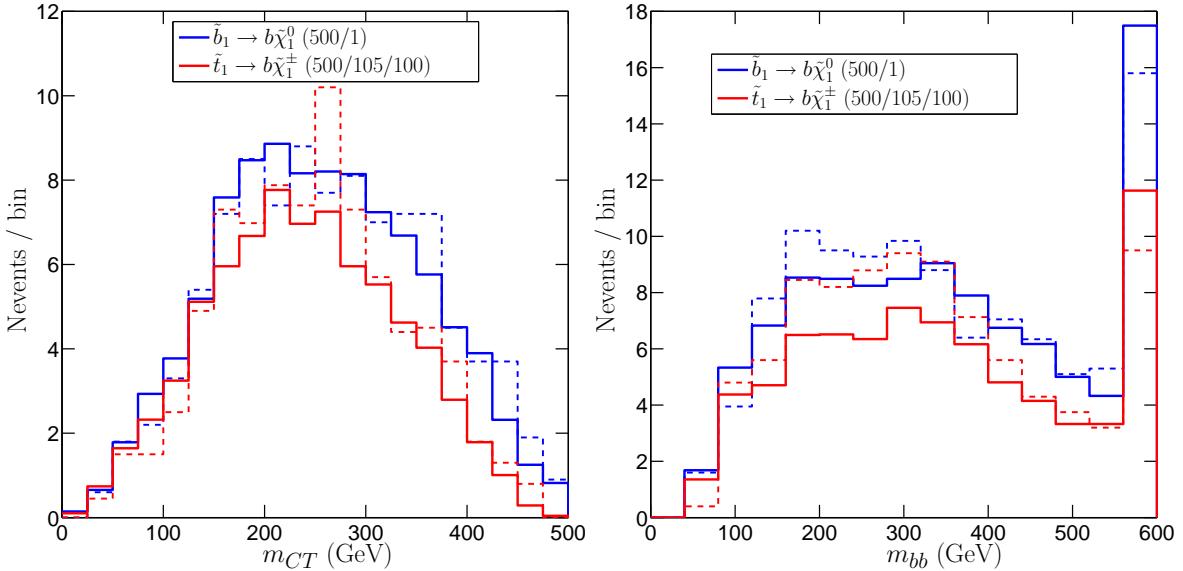


Figure 1: *Left*:  $M_{CT}$  distribution (in GeV) in *SRA* with all selection cuts except the  $M_{CT}$  requirement. *Right*:  $m_{bb}$  distribution (in GeV) with all selection cuts except the  $m_{bb}$  threshold. The solid line is the official plot and the dashed-dotted line is our own reimplementaion. The rightmost bins in the figures include the overflows.

### 3 Signal Region B (SRB)

The official distributions provided are the  $H_{T,3}$  and  $E_T^{\text{miss}}$  distributions.  $H_{T,3}$  is defined as the scalar sum of the  $p_T$  of the  $n$  jets, without including the three leading jets. The official plots display the  $H_{T,3}$  and  $E_T^{\text{miss}}$  distributions without their respective threshold. Using our own implementation the resulting plots are displayed in Figure 2. For this signal region there are discrepancies between the official analysis and our reimplementaion. For the  $H_{T,3}$  distribution (left panel of Figure 2), the region of interest will be the one where  $H_{T,3} < 50$  GeV, where we have the largest discrepancies, where our implementation is in excess with respect to the official one. The second bin is empty since reconstructed jets are required to have  $p_T > 20$  GeV (there is a 10 GeV binning). For the  $E_T^{\text{miss}}$  (right panel of Figure 2) our implementation also predicts an excess of events with respect to the official one, especially in the first bin of the left panel of Fig. 2). It seems that we have too many events with only three jets. However the agreement seems to be better for the 8TeV\_b300\_n200 benchmark point in the  $E_T^{\text{miss}}$  distribution and the largest discrepancies are found in the 8TeV\_t250\_c155\_n150 scenario. We now turn on the comparison with the official cutflows given in Table. 3 and Table. 4. These cutflows have been generated for the following benchmarks

$$SRB : \begin{cases} (m_{\tilde{b}_1}, m_{\tilde{\chi}_1^0}) = (350, 320) \text{ GeV} \\ (m_{\tilde{t}_1}, m_{\tilde{\chi}_1^\pm}, m_{\tilde{\chi}_1^0}) = (500, 420, 400) \text{ GeV} \end{cases} \quad (2)$$

$\tilde{b} \rightarrow b\tilde{\chi}_1^0$ (350/320) cutflow				
for SR $SRB$ , Low $\Delta M$ , $E_T^{\text{miss}} > 250$ GeV				
cut	# events (scaled to $\sigma$ and $\mathcal{L}$ )	relative change	# events (official)	relative change (official)
Initial number of events	16388.7	16388.7	16241	16241
$E_T^{\text{miss}} > 80$ GeV filter	5990.6	-63.4%	6221.0	6221.0
Lepton veto	4773.4	-20.3%	4069.0	-34.6%
$E_T^{\text{miss}} > 250$ GeV	790.5	-83.4%	757.0	-81.4%
Jet Selection	7.2	-99.1%	7.9	-99.0%
$H_{T,3} < 50$ GeV	6.0	-16.7%	5.2	-34.2%

Table 3: Cutflow for the benchmark point  $\tilde{b} \rightarrow b\tilde{\chi}_1^0$  (350/320) in the Signal Region  $SRB$ , Low  $\Delta M$ ,  $E_T^{\text{miss}} > 250$  GeV.

$\tilde{t} \rightarrow b\tilde{\chi}_1^\pm$ (500/420/400) cutflow				
for SR <i>SRB</i> , Low $\Delta M$ , $E_T^{\text{miss}} > 250$ GeV				
cut	# events (scaled to $\sigma$ and $\mathcal{L}$ )	relative change	# events (official)	relative change (official)
Initial number of events	1737.4	1737.4		
$E_T^{\text{miss}} > 80$ GeV filter	1109.9	-36.1%	1329.0	1329.0
Lepton veto	816.5	-26.4%	669.0	-49.7%
$E_T^{\text{miss}} > 250$ GeV	102.6	-87.4%	93.0	-86.1%
Jet Selection	4.7	-95.4%	6.2	-93.3%
$H_{T,3} < 50$ GeV	3.3	-29.8%	3.0	-51.6%

Table 4: Cutflow for the benchmark point  $\tilde{t} \rightarrow b\tilde{\chi}_1^\pm$  (500/420/400) in the Signal Region *SRB*, Low  $\Delta M$ ,  $E_T^{\text{miss}} > 250$  GeV. 100 000 signal events were generated for the cutflow.

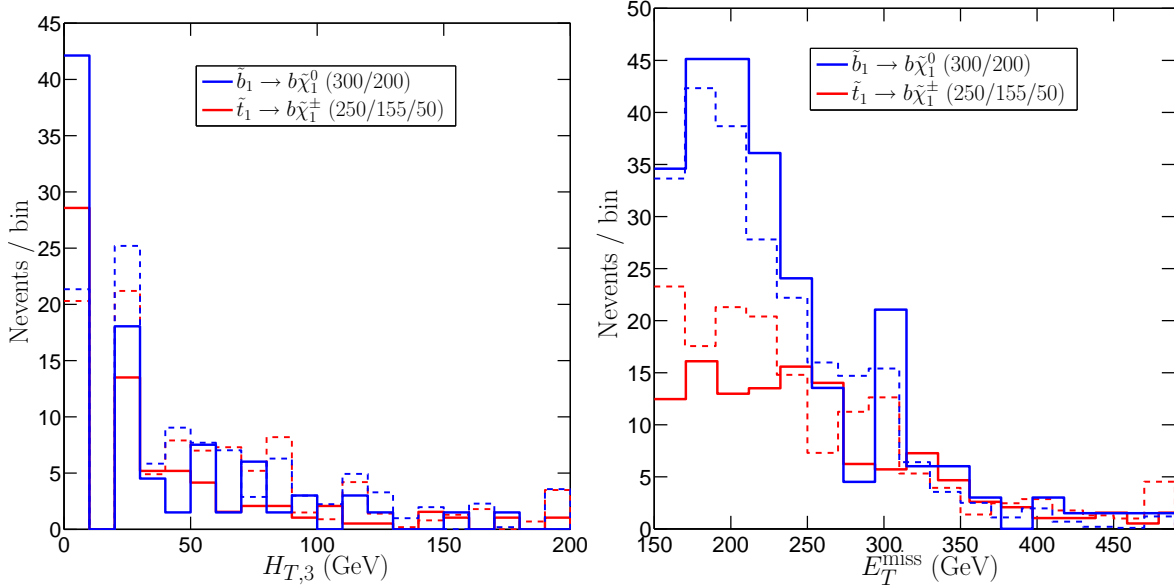


Figure 2: *Left*:  $H_{T,3}$  distribution (in GeV) in SRB with all selection cuts except the  $H_{T,3}$  requirement. *Right*:  $E_T^{\text{miss}}$  distribution (in GeV) with all selection cuts except the  $E_T^{\text{miss}}$  threshold. The solid line is the official plot and the dashed-dotted line is our own reimplementation. The rightmost bins in the figures include the overflows.

## 4 Limit-setting procedure

Limits are derived using `exclusion_CLs.py`. The 95% CL upper limits on the model cross section obtained from the code are compared to the ATLAS values [8] for the sbottom pair scenario considered in Fig. 3.

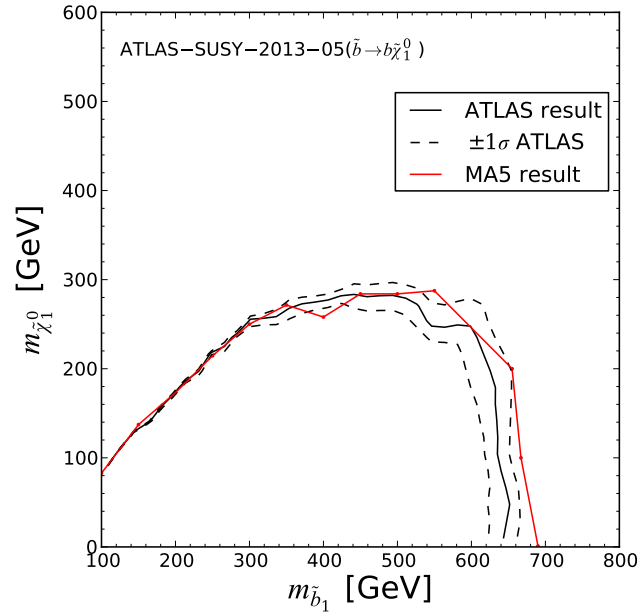


Figure 3: Comparison between the observed exclusion limit provided by ATLAS for the sbottom scenario against the recasted MA5 analysis. The black lines correspond respectively to the ATLAS result (the dashed lines correspond to the  $\pm 1\sigma$  theory uncertainty) and the red one to the MA5 one.

## References

- [1] G. Aad et al. (ATLAS), JHEP **1310**, 189 (2013), 1308.2631.
- [2] E. Conte, B. Fuks, and G. Serret, Comput.Phys.Commun. **184**, 222 (2013), 1206.1599.
- [3] J. Alwall, M. Herquet, F. Maltoni, O. Mattelaer, and T. Stelzer, JHEP **1106**, 128 (2011), 1106.0522.
- [4] J. de Favereau, C. Delaere, P. Demin, A. Giammanco, V. Lematre, et al. (2013), 1307.6346.
- [5] ATL-COM-PHYS-2013-1287.
- [6] D. R. Tovey, JHEP **0804**, 034 (2008), 0802.2879.
- [7] G. Polesello and D. R. Tovey, JHEP **1003**, 030 (2010), 0910.0174.
- [8] <https://atlas.web.cern.ch/Atlas/GROUPS/PHYSICS/PAPERS/SUSY-2013-05>.